Molecular recording of calcium signaling via calcium-dependent protein proximity labeling

Jungwoo Wren Kim[1], Adeline J. H. Yong[2,3], Ted M. Dawson[4], Valina L. Dawson[4], Yuh-Nung Jan[2,3], Nicholas T. Ingolia[1]

[1]Department of Molecular and Cell Biology, University of California, Berkeley, Berkeley, CA 94720, USA.

[2]Department of Physiology, University of California, San Francisco, San Francisco, CA 94158, USA

[3]Howard Hughes Medical Institute, University of California, San Francisco, San Francisco, CA 94158, USA

[4]Institute for Cell Engineering, Johns Hopkins University School of Medicine, Baltimore, MD 21205, USA.

Abstract

Calcium ions serve as key intracellular signals. Local, transient increases in calcium concentrations can activate calcium sensor proteins that in turn trigger downstream effectors. In neurons, calcium transients play a central role in regulating key neuronal processes including neurotransmitter release and synaptic plasticity. However, it is challenging to capture the molecular events associated with these localized and ephemeral calcium signals. Here we report the development of an engineered biotin ligase that combines the power of genetically encoded calcium indicators with protein proximity labeling. The enzyme, Cal-ID, biotinylates nearby proteins within minutes in response to elevated local calcium levels. The biotinylated proteins can be visualized by microscopy and identified via mass spectrometry. Cal-ID applied to mouse neurons showed increased biotinylation in active neurons, and mass spectrometry revealed active calcium signaling near Plasma Membrane Ca^{2+} ATPases. Therefore, we present Cal-ID as a biochemical recorder of calcium signaling and neuronal activity.

Introduction

Calcium ions (Ca^{2+}) are universal second messengers in eukaryotic cells. Ca^{2+} play essential roles in cellular physiology, and Ca^{2+} homeostasis is critical to cell viability. Cytosolic Ca^{2+} levels are typically maintained at ~100 nM, which is thought to be 10,000-fold lower than the extracellular Ca^{2+} levels[1]. However, cytosolic Ca^{2+} can increase rapidly due to influx through plasma membrane channels or release from intracellular stores. The resulting Ca^{2+} transients activate Ca^{2+} sensor proteins, which often bind to effector proteins in a Ca^{2+}-dependent manner to exert regulatory function. Ca^{2+} signaling is often localized to subcellular microdomains that form near the sites of Ca^{2+} influx as well, and thus can control both the position and timing of downstream responses[2].

Ca^{2+} signaling features prominently in neuronal physiology, where tight spatial and temporal control of signaling events is critical. Ca^{2+} regulates neurotransmitter release at the presynaptic active zone, and neurotransmitter receptors in turn allow Ca^{2+} influx into the postsynaptic region; additionally, G-protein-coupled neurotransmitter receptors trigger endoplasmic reticulum (ER)-mediated Ca^{2+} signaling[3]. Local Ca^{2+} dynamics play a key role in synaptic regulation, and activity-dependent gene expression requires Ca^{2+} signaling to the nucleus[4].

Indeed, Ca^{2+} dynamics can serve a valuable proxy of neuronal activity. Voltage-gated Ca^{2+} channels allow Ca^{2+} influx from the extracellular space when the plasma membrane depolarizes[5]. Therefore, chemical and genetic tools to monitor Ca^{2+} levels, such as Fura and Fluo dyes, and genetically encoded Ca^{2+} indicators such as GCaMPs, have been extensively

utilized to report on neuronal activity in real time[6]. These tools, which enabled researchers to track activities of many neurons via live imaging, became a landmark technological advance in neuroscience. However, they do not provide details about the molecular events occurring at the site of Ca^{2+} signaling events.

In the last decade, proximity labeling has emerged as a new approach for surveying macromolecular interaction and localization in living cells[7]. In proximity labeling, an engineered enzyme covalently modifies nearby proteins, often by generating diffusible but short-lived reactive compounds. For example, the *E. coli* Bifunctional ligase/repressor (BirA) has been adapted to promiscuously biotinylate proximal proteins by releasing an unstable intermediate[8,9]. Biotinylated proteins can then be identified via mass spectrometry, providing a powerful workflow for an unbiased, high-resolution mapping of protein-protein interaction. Importantly, proximity labeling captures these interactions in their biological context. We thus hypothesized that if proximal protein labeling could be done in a Ca^{2+}-dependent manner—with a labeling enzyme activated by elevated local Ca^{2+} levels—it would enable proteomic investigation of Ca^{2+} signaling microdomains.

In this study, we engineered a biotin ligase that switches conformation between inactive and active states depending on its Ca^{2+}-binding status. This enzyme, named Cal-ID, biotinylates nearby proteins when local Ca^{2+} levels are elevated. We expressed Cal-ID in HEK293T cells and investigated biotinylated proteins, allowing us to identify CEP131 and ASPM as primary components of the centrosomal Ca^{2+} signaling microdomain during mitosis. We also applied

Cal-ID to mouse primary cortical neurons and found that plasma membrane Ca^{2+} ATPases (PMCA) 1 and 2 occupy the most prominent Ca^{2+} signaling microdomains. These results highlight the value of Cal-ID as a novel and powerful tool that provides a new way to trace molecular events associated with Ca^{2+} signaling in cells.

Results

Development of Cal-ID, a Ca^{2+}-dependent, promiscuous biotinylation ligase

The genetically encoded Ca^{2+} indicator GCaMP functions via a Ca^{2+}-dependent conformational change that allows reversible intramolecular protein complementation of split green fluorescent protein (GFP). We envisioned that Ca^{2+}-dependent complementation of a split proximity labeling enzyme, instead of split GFP, would enable proximity protein labeling in response to elevated local Ca^{2+} levels. We chose the BioID labeling enzyme, which is an R118G mutant of the BirA biotin ligase, because it does not require any toxic or synthetic substrates and is proven to work in living mouse brain[10–12]. Based on the configuration of the genetically encoded calcium indicator GCaMP6s, we fused the Ca^{2+} sensor calmodulin and the Ca^{2+}-dependent calmodulin-binding peptide RS20 with circularly permuted, split BioID[13–15]. We expressed these fusions in HEK293T cells and found that a variant split between T195 and G196 has increased levels of promiscuous biotinylation when cytosolic Ca^{2+} levels were elevated by treatment with the sarco/endoplasmic reticulum Ca^{2+}-ATPase (SERCA) inhibitor thapsigargin (Extended Data Figs. 1a to 1c). Of note, this T195/G196 split site has not been tested in previous studies of split BirA variants[14–17]. Since this engineered enzyme successfully responded to elevated cytosolic Ca^{2+} levels in living cells, we named it Cal-ID (Calcium-dependent BioID).

Because Cal-ID labeling is irreversible, background levels of Ca^{2+} -independent activity pose a more serious challenge than background signal in fluorescence-based Ca^{2+} indicators. Biotinylated proteins may accumulate over extended labeling periods, or in response to high Cal-ID expression levels. Therefore, we set out to suppress activity of Cal-ID in the low-Ca^{2+} state and to enhance its signal-to-noise ratio. First, since a highly active, promiscuous BirA derivative called TurboID has been developed, we introduced the TurboID mutations to Cal-ID[8]. Next, we designed an inhibitory peptide, AviTag*—a non-biotinylatable and truncated variant of the wild-type BirA substrate peptide AviTag—that should block the enzyme active site. We fused this pseudosubstrate peptide to the N-terminus of Cal-ID, where it inhibits the enzyme in the absence of Ca^{2+}, yet be sequestered in response to Ca^{2+}-dependent calmodulin-RS20 binding (Fig. 1a). Indeed, we found that the N-terminal AviTag* fusion increased the Ca^{2+} responsiveness of Cal-ID during an extended 1-hour incubation in high extracellular biotin (Extended Data Fig. 2a). Last, a recent study reported a new split site, L73/G74, for protein-fragment complementation of TurboID[16]. We revised Cal-ID with this split site since the new split site variant shows prominent biotinylation only after a 15-min incubation (Extended Data Fig. 2b).

We then tested Ca^{2+}-dependent proximal biotinylation by this revised Cal-ID using various modes of cytosolic Ca^{2+} induction. In order to mimic the activity-dependent Ca^{2+} influx in neurons, we expressed the L-type voltage-gated calcium channel (L-VGCC) pore-forming alpha 1C subunit ($Ca_V1.2$) in HEK293T cells and showed that KCl depolarization triggers Cal-ID

biotinylation (Fig. 1c). We also showed that Ca^{2+} influx mediated by the Ca^{2+} ionophore ionomycin treatment also activates Cal-ID, similar to the effects of thapsigargin (Fig. 1d). Of note, we observed that replenishing serum in the culture media by adding fresh media to cells activates Cal-ID as well, suggesting that activation of signaling cascades triggering ER-mediated Ca^{2+} release can activate Cal-ID (Fig. 1d).

Cal-ID revealed cell cycle-dependent Ca^{2+} microdomains at centrosomes

Because TurboID has much higher activity than Cal-ID, it is not an ideal point of comparison for Cal-ID labeling experiments. We thus constructed cpTurboID, a circularly permuted TurboID without calmodulin or RS20, as a Ca^{2+}-independent control enzyme with labeling activity more similar to that of Cal-ID (Fig. 1b). cpTurboID is activated by spontaneous refolding, thereby providing a better control for the background activity of Cal-ID. It is also expected to reduce risks of potential cellular stress by depleting cellular biotin with extended incubation time, which occurs with highly reactive TurboID[8]. To compare these enzymes at defined expression levels, we generated stable HEK293T cell lines with tetracycline-inducible Cal-ID or cpTurboID expression via the Sleeping Beauty transposition and performed biotinylation experiments[18,19]. We found that cpTurboID has stronger yet comparable biotinylation levels to Cal-ID when they are expressed at similar levels and incubated for the same amount of time (Fig. 2a). In addition, we found that treatment of BAPTA-AM, a cell membrane-permeable form of the Ca^{2+} chelator BAPTA, reduces Cal-ID-mediated biotinylation but does not affect cpTurboID-mediated biotinylation in cells (Extended Data Fig. 2c). These results demonstrate that cpTurboID is a suitable Ca^{2+}-independent control for Cal-ID.

We next visualized the subcellular labeling pattern in Cal-ID-expressing cells and compared them with cpTurboID-expressing cells. cpTurboID biotinylation was observed throughout the cytosol, matching our expectations for a free and cytosolic promiscuous biotin ligase (Fig. 2b). In contrast, many Cal-ID-expressing cells showed distinctive, cell cycle-associated subcellular labeling patterns. In particular, mitotic Cal-ID-expressing cells showed strong biotinylation at the centrosome (Figs. 2b; see arrows, and 2c). Indeed, the importance of a Ca^{2+} microdomain in mitotic spindle formation is well established, and the elevated local Ca^{2+} concentration at the centrosome has been observed via genetically encoded Ca^{2+} indicators[20–23]. By detecting these well-studied Ca^{2+} microdomains, our results confirm that Cal-ID can detect physiologically relevant Ca^{2+} signaling events and demonstrate the spatial resolution of Ca^{2+}-dependent and proximal protein labeling by Cal-ID.

Quantitative proteomics identified Ca^{2+} signaling constituents in living cells

To investigate the distinct Cal-ID biotinylation patterns observed by microscopy in more detail, we wished to identify Cal-ID target proteins by proteomic mass spectrometry. Proximity labeling produces complex proteomic samples, but we and others have shown that ratiometric comparison of biotinylated samples can reveal specific patterns of biotinylation enrichment in the cell[24–26]. We thus carried out proximity labeling in Cal-ID- and cpTurboID-expressing cells and prepared samples for quantitative mass spectrometry with tandem mass tag (TMT) labeling for a ratiometric comparison of biotinylated proteins (Fig. 2d).

We detected 964 proteins overall and biological replicates showed high quantitative reproducibility in both labeling enzymes (r^2 > 0.98; Extended Data Figs. 3a and 3b, Supplementary Table 1). We then identified 29 proteins that were significantly enriched in Cal-ID relative to cpTurboID samples at 5% false discovery rate (FDR) and $\log_2$ fold change > 0.5 cutoff (Fig. 2e and Supplementary Table 1). The dramatic enrichment of calmodulin presumably reflects Cal-ID self-biotinylation and recovery of tryptic fragments from this fusion protein. Due to the sequence similarity, we cannot rule out the possibility that endogenous calmodulin is a major target of Cal-ID biotinylation and it could have contributed to the high enrichment of calmodulin as well. The second most enriched protein is CEP131, a centrosomal component protein. In addition to CEP131, ASPM, which is known to be associated with mitotic spindle regulation, is also significantly enriched by Cal-ID labeling[27]. This result is consistent with the strong Cal-ID biotinylation at centrosomes in mitotic cells. In addition, we found that 5 out of 29 top changes are from tubulin α- and β-subunits isoforms. Tubulins are the major component of the mitotic spindle, and β-Tubulin staining near the centrosome overlaps with fluorescent streptavidin staining (Fig. 3a). In addition, fluorescent streptavidin signal co-localizes with β-tubulin in multiple cell cycle stages, suggesting the general engagement of tubulins in Ca^{2+} microdomains (Extended Data Fig. 3c). Of note, we detected that Cal-ID localizes to the centrosome during mitosis and returns to cytosol during interphase, which is similar to the known localization of calmodulin along the cell cycle (Extended Data Fig. 3c)[28]. While these results suggest that Cal-ID localization is subject to the same regulatory mechanisms for calmodulin localization, we note that biotinylated Cal-ID proteins may have contributed to the strong streptavidin signal from centrosomes. In addition to CEP131, ASPM, and tubulins, Cal-ID

enriches several known Ca^{2+} signaling-associated proteins. These labeled proteins include IQGAP1, a Ras GTPase-like protein with IQ domains that bind to calmodulin, and MCU, a mitochondrial Ca^{2+} transporter involved in mitochondrial Ca^{2+} uptake[29,30]. We also saw enrichment of MYO6 and MYL6 myosin, which requires Ca^{2+} for its motor function. Finally, we identified FKBP7, an ER chaperone and thought to bind to Ca^{2+}, as its mouse ortholog has Ca^{2+}-binding affinity[31]. These results collectively show that Cal-ID combined with ratiometric quantitative proteomics can identify physiologically relevant Ca^{2+} signaling microdomains in living cells.

Cal-ID reported Ca^{2+} signaling-associated proteins at various subcellular regions

Since several Cal-ID target proteins identified by mass spectrometry have known subcellular localization, we performed additional immunostaining to investigate their potential co-localization with fluorescent streptavidin staining. When we performed immunostaining of FKBP7, an ER protein, we were able to find a subset of cells that show ER biotinylation patterns overlapping with FKBP7 (Fig. 3b). It is possible that these cells have active signaling cascades triggering Ca^{2+} release from the ER. In this regard, it is noteworthy that we also found cells that have increased cytosolic biotinylation and clustering of STIM1, which is a marker of activated store-operated Ca^{2+} entry (Extended Data Fig. 3d)[32]. Along with our observation that serum addition activates Cal-ID (Fig. 1d), we think that these observations are linked to activated Ca^{2+} signaling and Ca^{2+} release from the ER.

We identified Cal-ID enrichment of two nucleolar proteins, SURF6 and ZCCHC17. We immunostained SURF6, which showed higher enrichment than ZCCHC17, and found that SURF6 was strictly localized to the nucleolus in non-mitotic cells, although streptavidin signal was relatively weak in the nucleolus (Fig. 3c). However, during mitosis, SURF6 can be found in the cytosol and along the spindle fiber, suggesting that SURF6 biotinylation is mostly occurring during mitosis (Fig. 3c). While the function of human SURF6 in mitosis is not clear, yeast orthologs of SURF6 are known to be involved in spindle formation, which potentially explains SURF6 localization and biotinylation during mitosis[33]. In summary, ratiometric quantitative proteomics complements imaging in showing the ability of Cal-ID to record subcellular Ca^{2+} signaling microdomains in living cells.

Cal-ID biotinylation is associated with neuronal activity

In neurons, cytosolic Ca^{2+} influx from the extracellular space and release of Ca^{2+} from intracellular storage are key events in the regulation of neuronal function. Furthermore, neuronal activity is tightly associated with Ca^{2+} influx via various mechanisms including neurotransmitter receptors and voltage-gated Ca^{2+} channels[34]. We therefore set out to express Cal-ID in mouse primary neurons and test whether Cal-ID biotinylation is increased by neuronal activity. We delivered Cal-ID or cpTurboID to mouse primary cortical neurons by lentiviral transduction (Fig. 4a). To test how Cal-ID responds to neuronal activity, we silenced or activated the neuronal cultures and compared the overall Cal-ID biotinylation levels via western blot. We silenced neuronal cultures with NBQX and APV, which are antagonists of AMPA and NMDA glutamate receptors, respectively. For activation, we first silenced the culture and then treated

with $CaCl_2$ to induce neuronal activity[35]. We found that the extent of Cal-ID mediated biotinylation tracked with neuronal activity in the culture (Fig. 4b; see arrow).

To assess Ca^{2+}-dependent proximity labeling at a high resolution by fluorescence microscopy, we visualized Cal-ID biotinylation using streptavidin-conjugated fluorophores in primary hippocampal neurons. We again found that activated neuronal cultures showed higher overall biotinylation levels than silenced cultures (Fig. 4c). In order to investigate cell-to-cell variation in Cal-ID labeling within a single culture and correlate it with neuronal activity, we generated a Cal-ID-P2A-mScarlet-I fusion that synthesizes mScarlet-I co-translationally with Cal-ID and splits the two proteins into separate polypeptides by means of the P2A sequence. After Cal-ID labeling, we stained neurons to visualize a classic marker of neuronal activity, phospho-rpS6, along with biotinylation[36]. We found that mouse primary hippocampal neurons expressing Cal-ID showed a strong positive correlation between streptavidin and phospho-rpS6 signal intensity (Figs. 4d and 4e). The expression levels of the Cal-ID protein monitored by mScarlet-I did not show a similar correlation with phospho-rpS6, so the difference in biotinylation reflects greater Cal-ID activity in neurons with high phospho-rpS6 rather than greater abundance of the enzyme (Extended Data Fig. 4a). Similarly, we also found a positive correlation between phospho-CaMKII and streptavidin signals but not from phospho-CaMKII and mScarlet-I signals from mouse hippocampal neurons (Extended Data Figs. 4b and 4c). The results indicate that Cal-ID strategy is suitable to study neuronal activity-associated Ca^{2+} signaling microdomains in neurons.

Plasma membrane Ca^{2+} ATPases are the primary target of Cal-ID in mouse neurons

We showed that Cal-ID labeled proteins in HEK293T cells has distinctive subcellular biotinylation patterns (Fig. 2b) and wished to check whether the same held true in neurons. We first performed subcellular fractionation with mouse cortical neurons to ensure that Cal-ID and cpTurboID have comparable subcellular localization patterns in the neuron. Fractionation showed that both Cal-ID and cpTurboID localize and biotinylate proximal proteins at all major target regions including cytosolic, membranous, presynaptic, and postsynaptic regions (Extended Data Figs. 5a and 5b). We then expressed Cal-ID or cpTurboID in primary hippocampal neurons and compared their biotinylation patterns via microscopy. While both enzymes showed biotinylation across all components of the neuron, including the soma and the dendrites, fluorescent streptavidin staining revealed that Cal-ID-expressing cultures had more varying signal intensity levels between individual neurons compared to cpTurboID-expressing culture (Fig. 4f, top panel). In addition, active neurons labeled by Cal-ID have a strong, saturating level of signals that centered at the soma and often include primary branches, while the overall signal intensity is comparable to that seen in cpTurboID-labeled neurons (Fig. 4f, bottom panel).

We next sought to identify Cal-ID enriched proteins through a ratiometric proteomics comparison with cpTurboID. As in the experiment conducted with HEK293T cells, we prepared samples from mouse primary cortical neurons for quantitative mass spectrometry via TMT labeling. We measured expression of 669 proteins in this pulldown experiment, with high reproducibility ($r^2 > 0.92$) between biological replicates in both samples (Extended Data Figs. 6a

and 6b, Supplementary Table 1). We found 6 significantly enriched proteins by Cal-ID labeling at a 5% FDR (Fig. 5a). Calmodulin is again the most enriched protein by Cal-ID, reflecting Cal-ID self-biotinylation and potential biotinylation of endogenous calmodulin as discussed above. We found two plasma membrane Ca^{2+} ATPases (PMCA1 and PMCA2; *Atp2b1* and *Atp2b2*, respectively) from the list of 6 significantly enriched proteins. PMCAs play a role in maintaining Ca^{2+} homeostasis by pumping Ca^{2+} out from the cytoplasm[37,38]. The C-terminus of PMCAs is known to have multiple Ca^{2+} signaling-associated domains including calmodulin binding, high affinity Ca^{2+} binding for allosteric regulation, and a protein kinase C (PKC) target site[39,40]. In addition to PMCAs, we identified wolframin (*Wfs1*), an ER membrane protein known to be involved in Ca^{2+} homeostasis, as a target of Cal-ID. Mutations in *Wfs1* cause Wolfram syndrome, which is characterized by juvenile-onset insulin-dependent diabetes mellitus with optic atrophy, deafness, dementia, and psychiatric illness[41,42]. While the exact molecular mechanisms are unclear, it is thought to regulate ER Ca^{2+} levels in the context of ER-mitochondria crosstalk[43,44]. These top Cal-ID targets identified by mass spectrometry demonstrated the capacity of Cal-ID to detect Ca^{2+} signaling microdomain-associated proteins in neurons.

Proximity ligation assay provides selective imaging of Cal-ID targets

As PMCAs were identified as the top Cal-ID target proteins, we hypothesized that biotinylation of PMCAs may have contributed to the distinct streptavidin-fluorophore staining patterns in neurons expressing Cal-ID (Fig. 4f). Therefore, we sought to perform immunostaining of PMCAs and check their co-localization with streptavidin signals. However, the broad plasma membrane localization and high abundance of the PMCAs, as well as the presence of endogenous biotin

carrier proteins, posed a challenge to the interpretation of co-localization. We therefore turned to proximity ligation assays (PLA), which rely on very close (< 40 nm) co-localization of two different antibodies to create fluorescent signal (Fig. 5b)[45]. PLA between antibodies for biotin and the target protein provides a complementary method to confirm biotinylation of a specific target protein by Cal-ID and resolve its location more clearly.

To confirm the applicability of PLA to visualize biotinylation in neurons, we first examined self-biotinylation of Cal-ID and cpTurboID enzymes using anti-biotin antibodies along with anti-V5 antibodies against the V5 epitope tag on the biotin ligases. Consistent with the previous streptavidin imaging and western blot results, we found an even starker difference in biotinylation between naïve and stimulated neurons expressing Cal-ID, but not from cpTurboID-expressing neurons (Extended Data Figs. 6b and 6c). Next, we performed PLA with biotin and PMCA antibodies. We found that biotin-PLA signals from both PMCA1 and PMCA2 were significantly decreased when neuronal activity was suppressed (Fig. 5c to 5f). By focusing on biotin derived from proximity labeling and excluding endogenous biotin, PLA results verify that Cal-ID biotinylation is increased by neuronal activity.

Discussion

Ca^{2+} signaling is fundamental to cell physiology and widely conserved across eukaryotes. Most Ca^{2+} signals start from a transient increase of Ca^{2+} at a specific part of the cell[2]. While Ca^{2+} diffuses rapidly, elevated local Ca^{2+} concentration can be captured by Ca^{2+} sensor proteins and activate downstream signaling cascades. In this study, we exploited the function of the Ca^{2+}

sensor protein calmodulin to control the activity of a promiscuous biotin ligase in a Ca^{2+}-dependent manner. Since BirA-mediated biotinylation has a short labeling radius (~10 nm), this strategy enables us to biochemically label proteins near at the site where local Ca^{2+} levels are elevated (Fig. 6)[7]. Increased local Ca^{2+} occupies Ca^{2+} binding sites at calmodulin, shifting Cal-ID to the active, folded state via calmodulin-RS20 binding, thereby leading to proximal biotinylation. Once local Ca^{2+} levels drop to a resting state, calmodulin will release Ca^{2+}, disrupting the interaction with RS20 and allowing the Cal-ID to return to an inactive conformation. This conformational cycle places a permanent covalent mark on proximal proteins in response to transient changes in local Ca^{2+} concentration.

Cal-ID labeling in HEK293T cells highlighted Ca^{2+} signaling microdomains at the mitotic centrosome. The necessity of local Ca^{2+} signaling for mitotic spindle formation has been known for decades, which is in good alignment with our observation of strong Cal-ID biotinylation at the centrosome. It is noteworthy that, while multiple pericentriolar proteins such as pericentrin (PNCT) and AKAP450 contain potential calmodulin-binding motifs, the primary proteins constituting centrosomal Ca^{2+} signaling microdomains have not been identified[46,47]. Our Cal-ID mass spectrometry results implicated CEP131 and ASPM—both of which contain a calmodulin-binding IQ domain—as key components for centrosomal Ca^{2+} signaling. Potential Ca^{2+}-dependent roles of CEP131 and ASPM in mitotic spindle regulation could expand our knowledge of Ca^{2+} signaling events at the centrosome.

We observed that Cal-ID localization in mitotic cells is similar to the previously reported calmodulin distribution during mitosis (Fig. 3a)[28]. This suggests that, when Cal-ID is expressed freely in the cytoplasm, the calmodulin component of the fusion could affect its localization. While this localization could facilitate identification of endogenous Ca^{2+} signaling microdomains mediated by calmodulin, it is also possible that proteins with calmodulin-binding motifs are preferred by Cal-ID even when Cal-ID is targeted to regions of interest. Since many calmodulin-binding partners have Ca^{2+}-dependent binding affinity, and most calmodulin-associated molecular processes are involved in Ca^{2+}-dependent regulation, we believe that the possibility of identifying false positives due to calmodulin-binding affinity is low[48]. However, we suggest that Cal-ID labeling results should be interpreted in consideration of the existence of calmodulin-binding motifs.

In neurons, Ca^{2+} signaling is associated with neuronal activity and plays an essential role in activity-dependent regulation[4]. At synapses, Ca^{2+} influx via neurotransmitter receptors, Ca^{2+} channels, and release of ER-stored Ca^{2+} is a central part for local synaptic regulation in both short- and long-term. Ca^{2+} signaling back to the nucleus is essential for the expression of activity-dependent gene expression. We therefore expect that identifying Ca^{2+} microdomain constituents via Cal-ID will hold a particular value in our understanding on the molecular physiology of the neuron. In primary cortical neurons, Cal-ID labeling enriches Atp2b1 (PMCA1) and Atp2b2 (PMCA2)—major Ca^{2+} pumps which are responsible for extruding cytosolic Ca^{2+}. The high abundance of PMCAs in neurons and their affinity to calmodulin may contribute to their Cal-ID labeling. However, there are other abundant neuronal proteins with known

calmodulin-binding motifs, such as voltage-gated Ca^{2+} channels and ryanodine receptors, which drive major Ca^{2+} influx into cytoplasm in neurons[34]. Therefore, it is plausible to speculate that high local Ca^{2+} concentrations and Ca^{2+} signaling microdomains are maintained around PMCAs, since active export is relatively slower than Ca^{2+} influx through channels. In addition, our results help to identify the subcellular location of fluorescent signals generated by genetically encoded Ca^{2+} indicators that incorporate calmodulin, such as GCaMPs. Further investigation of the Ca^{2+} signaling events around PMCAs is warranted to expand our understanding on the formation and regulation of Ca^{2+} microdomains in neurons.

Cal-ID labeling and imaging could be especially advantageous in neuroscience as an approach to track neuronal activity. Prominent PMCA labeling facilitates visualization of Cal-ID-labeled neurons. Cal-ID biotinylation reaches to a detectable level by streptavidin imaging between 0.5 – 1 hour, which is significantly faster than transcription-based methods for active neuron labeling. Furthermore, the high spatial resolution and the biochemical nature of proximity labeling enables Cal-ID to record Ca^{2+} microdomains at a brain-wide scale. This approach may offer distinctive advantages over other tools such as CaMPARI, a photoactivatable Ca^{2+} indicator[49,50]. While CaMPARI can 'mark' neuronal activity at a great temporal resolution, the need for light activation limits the maximum area of recording. However, enzymatic Cal-ID labeling will be much slower than the millisecond timescale of CaMPARI, which must be considered when interpreting these data.

More broadly, Cal-ID differs in important ways from fluorescent Ca^{2+} indicators. Cal-ID functions on a different timescale and may require incubation over many minutes to accumulate detectable signals. Therefore, while Cal-ID is activated by Ca^{2+} transients, Cal-ID biotinylation is not necessarily representing a single Ca^{2+} transient. Visualization of Cal-ID biotinylation may benefit from the amplification and specificity offered by PLA or other approaches, because endogenous biotin carrier proteins give background biotin signals from mitochondria. Additionally, it has been reported that ectopic expression of Ca^{2+}-binding proteins in fluorescent indicators can alter Ca^{2+} buffering, and Cal-ID may have similar limitations[51].

In this study, we presented Cal-ID, an engineered proximal protein ligase that is activated by Ca^{2+}-dependent refolding. Cal-ID functions as a molecular recorder of Ca^{2+} microdomains, thereby providing a unique way to investigate Ca^{2+} signaling events in living cells. We suggest that Cal-ID has great application potentials in multiple fields of biology that cellular activation accompanied by Ca^{2+} influx is important, such as neuroscience and immunology.

Methods

Cloning

See Supplementary Table 2 for the key constructs used in this study. For cloning, PCR primers were designed to have overhangs, PCR reactions were performed with Q5 polymerase (New England BioLabs, NEB), and the fragments were assembled using HiFi (NEB) or Gibson assembly (NEB). Ligated plasmid products were introduced by heat shock transformation into competent Stbl3 (Invitrogen). The cloning products were confirmed using Sanger sequencing. Calmodulin

and RS20 sequences were derived from GCaMP6s[13]. All biotin ligase variants were derived from E. coli biotin protein ligase, from BioID or TurboID[8,9].

HEK293T Cell Culture and Generation of Stable Cell Lines

HEK293T cells were maintained with DMEM with GlutaMax (Gibco) supplemented with 10% tetracycline-free FBS (Gibco). Cal-ID and cpTurboID transgenes were cloned into the pSBtet-Hyg (Addgene #60508) donor vector, mixed at a 5:1 ratio with pCMV(CAT)T7-SB100 (Addgene #34879), and co-transfected to HEK293T cells using TransIT-293 (Mirus). 48 hours after transfection, 200 µg/mL hygromycin (Invitrogen) was added to the culture medium and selected for 3 passages each with a 1:20 split ratio.

Primary Neuron Culture

Dissociated primary cortical neurons were prepared from E15 developing brain (CD1, Charles River). Developing cortices were dissected in dissecting medium (Dulbecco's Modified Eagle Medium (DMEM) with 20 % FBS, 0.5 mM GlutaMax, 6 µM glucose, Gibco), digested with 20 mg/ml papain (Worthington) for 20 min at 37 °C, and plated at a concentration of 1.2×10^6 cells for a 12-well plate (cortical neurons) or 60,000 – 70,000 neurons per one well of 24-well plate (hippocampal neurons), 4.2×10^6 cells per 100 mm dish, 7×10^6 cells per 150 mm dish. Culture plates were pre-coated with 50 µg/mL poly-D-lysine. Cultures were maintained under Neurobasal Plus (Gibco) medium with a serum-free supplement B-27 plus (Gibco) and 0.5mM GlutaMax (Gibco).

Immunocytochemistry

Cells were washed 3 times and fixed with 4 % paraformaldehyde for 15 min at RT, washed 3 times again then permeabilized and blocked for 1 hour with 5 % BSA and 0.1 % saponin in PBS. The blocked cells were subsequently incubated with primary antibody overnight at 4 °C. On the following day, the cells were washed 3 times and incubated with secondary antibody for 1 hour at room temperature in a light controlled condition. After 3 × wash with PBS buffer, the cells were mounted on cover slides with mounting media containing DAPI (VECTASHIELD® Plus, Vector Labs, H-1900). All images were taken for analysis with LSM710 (Carl Zeiss) confocal laser scanning microscope under 20 × air or 63 × oil objectives or SP8 (Leica) confocal laser scanning microscope with a 40 × oil objective. See Supplementary Table 2 for the antibodies used in this study.

Immunoblotting

Brain tissues were lysed with an automated homogenizer in RIPA buffer with 1 % SDS (20 mM Tris-HCl (pH 7.4), 150 mM NaCl, 1 mM EDTA, 1 % NP-40, 1 % sodium deoxycholate, 1 % SDS, protease inhibitors). Lysates were incubated on a rotator for 1 hour at 4 °C, and debris was separated by centrifugation for 10 min × 12,000 g at 4 °C. Supernatant was collected, protein concentration was measured, and the lysate was mixed with 2 × Laemmli sample buffer. SDS-PAGE and transfer were performed on Invitrogen Bolt™ system with Bis-Tris 4-12% gradient gels. ProteinSimple or Li-Cor imager was used for visualization. See Supplementary Table 2 for the antibodies used in this study.

Lentivirus generation

Cal-ID or cpTurboID transgenes were cloned into pJW1511 (Addgene #62365) or FUGW (Addgene #14883) transfer vectors after removing the original transgene. Transfer vectors were co-transfected into low passage number (< 15) HEK293T cells with 3rd generation VSV-G and gag/pol plasmids at a 1:2:3 ratio. 1 day after transfection culture, media was replaced with new media with 10 mM (final) HEPES. The first harvest of packaged virus was made 2 days after transfection, mixed with Lenti-X concentrator (Takara), and stored at 4°C. A second harvest was made 3 days after transfection, mixed with Lenti-X concentrator and concentrated along with the first harvest following the manufacturer's recommendation. The relative titer of the lentiviral concentrate was estimated using Lenti-X GoStix (Takara).

Sample preparation for Mass Spectrometry

Samples for mass spectrometry were prepared following the previously published protocol for proteomics analysis of TurboID-labled proteins from Alice Ting's laboratory[52]. Briefly, 2 × 150 mm dishes of cells were used for each sample. Biological replicates were prepared for both cpTurboID and Cal-ID labeling. For inducible HEK293T cell lines, 400 ng/mL doxycycline was used for Cal-ID induction and 200 ng/mL doxycycline was used for cpTurboID induction, each for 48 hours. For lentiviral transduction, concentrated lentiviral titer was estimated by Takara GoStix and GV ~25,000 (cpTurboID) or ~50,000 (Cal-ID) viruses were applied to neuronal cultures at 1:50 volume ratio. For biotinylation, 100 µM biotin was added and incubated for 1 hour in tissue culture incubator. Cells were washed with ice-cold PBS with 5 times and lysed with 1.5 mL RIPA lysis buffer (50 mM Tris, 150 mM NaCl, 0.1 % (wt/vol) SDS, 0.5 % (wt/vol)

sodium deoxycholate, 1 % (vol/vol) Triton X-100, pH 7.4). 2.5 % of lysates were saved and further analyze by western blot to ensure biotinylation of the samples. The samples were incubated with 250 µl magnetic streptavidin beads (Thermo Fisher Scientific) at 4 °C overnight with rotation. The beads were washed twice with RIPA buffer (1 mL, 2 min at RT), once with 1 M KCl (1 mL, 2 min at RT), once with 0.1 M Na_2CO_3 (1 mL, ~10 s), once with 2 M urea in 10 mM Tris-HCl (pH 8.0) (1 mL, ~10 s), and twice with RIPA buffer (1 mL per wash, 2 min at RT). 2.5% of the beads were analyzed by silver staining to ensure successful pulldown of biotinytlated proteins. The beads were washed again with 200 µL of 50 mM Tris-HCl (pH 7.4), twice with 200 µL 2M urea in 50 mM Tris (pH 7.4) buffer. Then the beads were incubated with 80 µL of 2 M urea in 50 mM Tris-HCL containing 1 mM DTT and 0.4 µg trypsin (Promega) at 25 °C for 1 hour while shaking at 1,000 rpm. The supernatant containing digested peptides was saved, and beads were washed twice with 60 µL of 2 M urea in 50 mM Tris (pH 7.4) buffer and combined the washes with the digestion supernatant. DTT was added to a final concentration of 4 mM and incubated with the eluate at 25 °C for 30 min with shaking at 1,000 rpm. The samples were alkylated by iodoacetamide to a final concentration of 10 mM and incubated at 25 °C for 45 min with 1,000 rpm agitation, protected from light. 0.5 µg of trypsin was added to the samples and further digested overnight at 25 °C with shaking at 700 rpm. The next day, formic acid was added at ~1 % (vol/vol) to adjust sample pH to ~ 3. Samples were desalted using C18 StageTips as previously described[53].

TMT labeling and quantitative mass spectrometry

Peptides were quantified and normalized using a quantitative colorimetric peptide assay (Thermo Fisher Scientific). TMT reagents were reconstituted with 41 µL of anhydrous acetonitrile with occasional vortexing for 5 min at RT. The reduced and alkylated proteins were transferred to the TMT vials and incubated for 1 hour at RT. The reaction was quenched with addition of 8 µL of 5% hydroxyamine and incubation for 15 min. The samples were desalted with C18 StageTips. Samples were run on an OrbiTrap mass spectrometer (ThermoFisher Scientific) using high pH fractionation.

Mass Spectrometry Data Analysis

Mass spectra were processed using Proteome Discoverer (Thermo Scientific). Quantitative mass spectrometry results were analyzed using limma (3.34.9) in R[54]. Proteins with no peptide detected from any condition were omitted. Pre-normalization raw intensity values were transformed by the voom function, and the values were fitted for linear models via limma to estimate differential representation of proteins in Cal-ID vs cpTurboID pull-down samples with biological replicates. FDR was calculated by Benjamini-Hochberg correction.

Proximity Ligation Assay

Proximity Ligation Assay (PLA) was performed using Duolink® (MilliporeSigma, DUO92101) following the manufacturer's protocol. Briefly, mouse hippocampal neurons were fixed with 4 % paraformaldehyde for 15 minutes at RT, then permeabilized with 0.1% Triton X-100 for 15 min. The cells were washed then blocked for 1 hour at 37 °C with a humidity chamber with the Duolink® Blocking Solution. The blocked cells were subsequently incubated with primary

antibodies diluted with the Duolink® Antibody Diluent (conditions are below) overnight at 4°C. The following day, cells were washed twice with Wash A buffer for 5 min at RT. Duolink® PLUS and MINUS probes were diluted with the Diluent with 1:5 concentration, added to the coverslips, incubated at 37 °C for 1 hour in a humidity chamber. After incubation, the coverslips were washed twice with Wash A buffer for 5 min at RT. When any additional secondary antibodies were used in addition to the PLA probes, secondary antibodies in the Diluent were added and incubated for 40 mins at 37 °C, and washed with Wash A buffer twice for 5 min. After that, 1 × Duolink® Ligation buffer was prepared, ligase was added following 1:40 ratio, mixed well and added to the coverslips. The ligation reaction was performed for 30 min at 37 °C in a humidity chamber. Following ligation, coverslips were washed twice with Wash A buffer, and 1 × Amplification reaction mix with 1:80 enzyme:buffer ratio was prepared and added. The amplification reaction was performed for 100 min at 37 °C in a humidity chamber. Final wash was performed with 1 × Wash B buffer twice for 10 min then 0.01 × Wash B buffer once for 1 min. The coverslips were mounted using VECTASHIELD PLUS® (Vector Labs) or Duolink® DAPI mounting solution provided with the kit. See Supplementary Table 2 for the antibodies used for the experiments.

Image Analysis

For streptavidin and P-S6/P-CaMKII correlation and PLA analyses, ImageJ (1.53f51)/FIJI was used[55]. Cell bodies of the mScarlet-I expressing neurons were selected via Threshold, Watershed, and Analyze Particles tools with 50 – infinity size selection in ImageJ. Cells on the edges were excluded. After selecting soma regions, target mean intensity values were extracted

from the selections and transferred to R. The results were analyzed in R and visualized using ggplot2 (3.0.0)[56]. The heatmap was generated by Calibration Bar tool in ImageJ.

Subcellular Fractionation

Samples were kept on ice during the procedure and centrifugations and incubations were conducted at 4 °C. All solutions contained phosphatase inhibitors (Sigma-Aldrich PhosSTOP™), protease inhibitors (Roche cOmplete™), 5 mM sodium pyrophosphate, 1 mM EDTA, and 1 mM EGTA. Cultured cortical neurons were collected by scraping and homogenizing by passage through a 26G needle 12 times, in homogenization buffer (320 mM sucrose, 10 mM HEPES). The homogenate was centrifuged at 800 g for 10 min to obtain the post-nuclear pelleted fraction 1 (P1) and supernatant fraction 1 (S1). S1 was further centrifuged at 15,000 g for 20 min to yield P2 (membranous fraction) and S2 (cytosolic fraction). P2 was resuspended in Milli-Q® water, adjusted to 4 mM HEPES (pH 7.4), and incubated with agitation for 30 min before centrifugation at 25,000 g for 20 min to obtain LP1 (mitochondria, pre- and postsynaptic membranes) and LS2 (synaptosomal cytosolic fraction). LP1 was resuspended in 50 mM HEPES (pH 7.4), mixed with an equal volume of 1 % Triton X-100, and incubated with agitation for 8 min. Lastly, centrifugation at 25,000 g for 20 min yielded the presynaptic membranes (supernatant) and the postsynaptic density (pellet).

Acknowledgements

We thank S. Eacker and members of the Ingolia and the Lareau labs for discussion. Mass spectrometry was conducted at the UC Davis Proteomics Core. Confocal imaging was conducted at the CRL Molecular Imaging Center, RRID:SCR_017852, supported by Gordon and Betty Moore Foundation. **Funding:** This work was supported by FRAXA Fragile X Foundation Postdoctoral Fellowship (J.W.K.), NIH NCI DP2CA195768 (N.T.I.), and NINDS R21NS112842 (N.T.I.). **Author contributions:** J.W.K. and N.T.I. conceived the study and designed the experiments. J.W.K., A.J.H.Y. conducted the experiments. J.W.K. and N.T.I. analyzed proteomics data. Y.N.J. supervised biochemistry and microscopy experiments with neurons. T.M.D. and V.L.D. oversaw conceptualization of the study. J.W.K. and N.T.I. wrote the manuscript with input from all authors. **Competing interests**: The authors declare no competing interests. **Data and materials availability**: Plasmids and libraries will be available through Addgene. All source code used for data analysis will be available upon request.

Supplementary Information

Supplementary Data Table 1. TMT mass spectrometry results table

Supplementary Data Table 2. Key constructs and antibodies used for the study

References

1. Bagur, R. & Hajnóczky, G. Intracellular Ca2+ Sensing: Its Role in Calcium Homeostasis and Signaling. *Molecular Cell* 66, 780–788 (2017).

2. Berridge, M. J. Calcium microdomains: Organization and function. *Cell Calcium* 40, 405–412 (2006).

3. Augustine, G. J., Santamaria, F. & Tanaka, K. Local calcium signaling in neurons. *Neuron* 40, 331–346 (2003).

4. Greer, P. L. & Greenberg, M. E. From Synapse to Nucleus: Calcium-Dependent Gene Transcription in the Control of Synapse Development and Function. *Neuron* 59, 846–860 (2008).

5. Simms, B. A. & Zamponi, G. W. Neuronal voltage-gated calcium channels: structure, function, and dysfunction. *Neuron* 82, 24–45 (2014).

6. Lin, M. Z. & Schnitzer, M. J. Genetically encoded indicators of neuronal activity. *Nature Neuroscience* 19, 1142–1153 (2016).

7. Qin, W., Cho, K. F., Cavanagh, P. E. & Ting, A. Y. Deciphering molecular interactions by proximity labeling. *Nat Methods* 18, 133–143 (2021).

8. Branon, T. C. *et al.* Efficient proximity labeling in living cells and organisms with TurboID. *Nat Biotechnol* 36, 880–887 (2018).

9. Roux, K. J., Kim, D. I., Raida, M. & Burke, B. A promiscuous biotin ligase fusion protein identifies proximal and interacting proteins in mammalian cells. *J. Cell Biol.* 196, 801–810 (2012).

10. Han, S., Li, J. & Ting, A. Y. Proximity labeling: spatially resolved proteomic mapping for neurobiology. *Curr Opin Neurobiol* 50, 17–23 (2018).

11. Uezu, A. & Soderling, S. Identifying Synaptic Proteins by In Vivo BioID from Mouse Brain. *Methods Mol Biology Clifton N J* 2008, 107–119 (2019).

12. Uezu, A. *et al.* Identification of an elaborate complex mediating postsynaptic inhibition. *Science* 353, 1123–1129 (2016).

13. Chen, T.-W. *et al.* Ultrasensitive fluorescent proteins for imaging neuronal activity. *Nature* 499, 295–300 (2013).

14. Schopp, I. M. *et al.* Split-BioID a conditional proteomics approach to monitor the composition of spatiotemporally defined protein complexes. *Nat Commun* 8, 1–14 (2017).

15. Munter, S. D. *et al.* Split-BioID: a proximity biotinylation assay for dimerization-dependent protein interactions. *FEBS Lett.* 591, 415–424 (2017).

16. Cho, K. F. *et al.* Split-TurboID enables contact-dependent proximity labeling in cells. *Proc Natl Acad Sci USA* 17, 201919528–12 (2020).

17. Kwak, C. *et al.* Contact-ID, a tool for profiling organelle contact sites, reveals regulatory proteins of mitochondrial-associated membrane formation. *Proc. Natl. Acad. Sci. U.S.A.* 265, 201916584 (2020).

18. Davidson, A. E., Gratsch, T. E., Morell, M. H., O'Shea, K. S. & Krull, C. E. Use of the Sleeping Beauty transposon system for stable gene expression in mouse embryonic stem cells. *Cold Spring Harb Protoc* 2009, pdb.prot5270-pdb.prot5270 (2009).

19. Kowarz, E., Löscher, D. & Marschalek, R. Optimized Sleeping Beauty transposons rapidly generate stable transgenic cell lines. *Biotechnol J* 10, 647–653 (2015).

20. Helassa, N., Nugues, C., Rajamanoharan, D., Burgoyne, R. D. & Haynes, L. P. A centrosome-localized calcium signal is essential for mammalian cell mitosis. *The FASEB Journal* 33, 14602–14610 (2019).

21. Whitaker, M. Calcium microdomains and cell cycle control. *Cell Calcium* 40, 585–592 (2006).

22. Groigno, L. & Whitaker, M. An Anaphase Calcium Signal Controls Chromosome Disjunction in Early Sea Urchin Embryos. *Cell* 92, 193–204 (1998).

23. Lagos-Cabré, R., Ivanova, A. & Taylor, C. W. Ca2+ Release by IP3 Receptors Is Required to Orient the Mitotic Spindle. *Cell Rep* 33, 108483 (2020).

24. Fazal, F. M. *et al.* Atlas of Subcellular RNA Localization Revealed by APEX-Seq. *Cell* 178, 473-490.e26 (2019).

25. Padrón, A., Iwasaki, S. & Ingolia, N. T. Proximity RNA Labeling by APEX-Seq Reveals the Organization of Translation Initiation Complexes and Repressive RNA Granules. *Molecular Cell* 75, 875-887.e5 (2019).

26. Qin, W., Myers, S. A., Carey, D. K., Carr, S. A. & Ting, A. Y. Spatiotemporally-resolved mapping of RNA binding proteins via functional proximity labeling reveals a mitochondrial mRNA anchor promoting stress recovery. *Nat Commun* 12, 4980 (2021).

27. Zhong, X., Liu, L., Zhao, A., Pfeifer, G. P. & Xu, X. The abnormal spindle-like, microcephaly-associated (ASPM) gene encodes a centrosomal protein. *Cell Cycle Georget Tex* 4, 1227–9 (2005).

28. Li, C. J. *et al.* Dynamic redistribution of calmodulin in HeLa cells during cell division as revealed by a GFP-calmodulin fusion protein technique. *J Cell Sci* 112, 1567–1577 (1999).

29. Hart, M. J., Callow, M. G., Souza, B. & Polakis, P. IQGAP1, a calmodulin-binding protein with a rasGAP-related domain, is a potential effector for cdc42Hs. *Embo J* 15, 2997–3005 (1996).

30. Mammucari, C., Gherardi, G. & Rizzuto, R. Structure, Activity Regulation, and Role of the Mitochondrial Calcium Uniporter in Health and Disease. *Frontiers Oncol* 7, 139 (2017).

31. Zhang, X. *et al.* The mouse FKBP23 binds to BiP in ER and the binding of C-terminal domain is interrelated with Ca2+ concentration. *Febs Lett* 559, 57–60 (2004).

32. Park, C. Y. *et al.* STIM1 Clusters and Activates CRAC Channels via Direct Binding of a Cytosolic Domain to Orai1. *Cell* 136, 876–890 (2009).

33. Oeffinger, M., Fatica, A., Rout, M. P. & Tollervey, D. Yeast Rrp14p is required for ribosomal subunit synthesis and for correct positioning of the mitotic spindle during mitosis. *Nucleic Acids Res* 35, 1354–1366 (2007).

34. Berridge, M. J. Neuronal Calcium Signaling. *Neuron* 21, 13–26 (1998).

35. Leitz, J. & Kavalali, E. T. Ca^{2+} influx slows single synaptic vesicle endocytosis. *J Neurosci Official J Soc Neurosci* 31, 16318–26 (2011).

36. Knight, Z. A. *et al.* Molecular Profiling of Activated Neurons by Phosphorylated Ribosome Capture. *Cell* 151, 1126–1137 (2012).

37. Garcia, M. L. & Strehler, E. E. Plasma membrane calcium ATPases as critical regulators of calcium homeostasis during neuronal cell function. *Front Biosci* 4, d869 (1999).

38. Strehler, E. E. Plasma membrane calcium ATPases: From generic Ca2+ sump pumps to versatile systems for fine-tuning cellular Ca2+. *Biochem Bioph Res Co* 460, 26–33 (2015).

39. STREHLER, E. E. *et al.* Plasma Membrane Ca2+ ATPases as Dynamic Regulators of Cellular Calcium Handling. *Ann Ny Acad Sci* 1099, 226–236 (2007).

40. Brini, M. & Carafoli, E. The Plasma Membrane Ca2+ ATPase and the Plasma Membrane Sodium Calcium Exchanger Cooperate in the Regulation of Cell Calcium. *Csh Perspect Biol* 3, a004168–a004168 (2010).

41. Yurimoto, S. *et al.* Identification and characterization of wolframin, the product of the wolfram syndrome gene (WFS1), as a novel calmodulin-binding protein. *Biochemistry* 48, 3946–3955 (2009).

42. Osman, A. A. *et al.* Wolframin Expression Induces Novel Ion Channel Activity in Endoplasmic Reticulum Membranes and Increases Intracellular Calcium*. *J Biol Chem* 278, 52755–52762 (2003).

43. Angebault, C. *et al.* ER-mitochondria cross-talk is regulated by the Ca2+ sensor NCS1 and is impaired in Wolfram syndrome. *Science Signaling* 11, (2018).

44. Morgia, C. L. *et al.* Calcium mishandling in absence of primary mitochondrial dysfunction drives cellular pathology in Wolfram Syndrome. *Scientific Reports* 10, 4785 (2020).

45. Söderberg, O. *et al.* Direct observation of individual endogenous protein complexes in situ by proximity ligation. *Nat Methods* 3, 995–1000 (2006).

46. Gillingham, A. K. & Munro, S. The PACT domain, a conserved centrosomal targeting motif in the coiled-coil proteins AKAP450 and pericentrin. *Embo Rep* 1, 524–529 (2000).

47. Moisoi, N., Erent, M., Whyte, S., Martin, S. & Bayley, P. M. Calmodulin-containing substructures of the centrosomal matrix released by microtubule perturbation. *J Cell Sci* 115, 2367–79 (2002).

48. Chin, D. & Means, A. R. Calmodulin: a prototypical calcium sensor. *Trends Cell Biol* 10, 322–328 (2000).

49. Fosque, B. F. *et al.* Labeling of active neural circuits in vivo with designed calcium integrators. *Science* 347, 755–760 (2015).

50. Trojanowski, N. F., Bottorff, J. & Turrigiano, G. G. Activity labeling in vivo using CaMPARI2 reveals intrinsic and synaptic differences between neurons with high and low firing rate set points. *Neuron* 109, 663-676.e5 (2021).

51. McMahon, S. M. & Jackson, M. B. An Inconvenient Truth: Calcium Sensors Are Calcium Buffers. *Trends Neurosci* 41, 880–884 (2018).

52. Cho, K. F. *et al.* Proximity labeling in mammalian cells with TurboID and split-TurboID. *Nature Protocols* 92, 1–31 (2020).

53. Rappsilber, J., Mann, M. & Ishihama, Y. Protocol for micro-purification, enrichment, pre-fractionation and storage of peptides for proteomics using StageTips. *Nature Protocols* 2, 1896–1906 (2007).

54. Ritchie, M. E. *et al.* limma powers differential expression analyses for RNA-sequencing and microarray studies. *Nucleic Acids Res* 43, e47–e47 (2015).

55. Schindelin, J. *et al.* Fiji: an open-source platform for biological-image analysis. *Nat Methods* 9, 676–682 (2012).

56. Wickham, H. ggplot2, Elegant Graphics for Data Analysis. 147–168 (2016) doi:10.1007/978-3-319-24277-4_7.

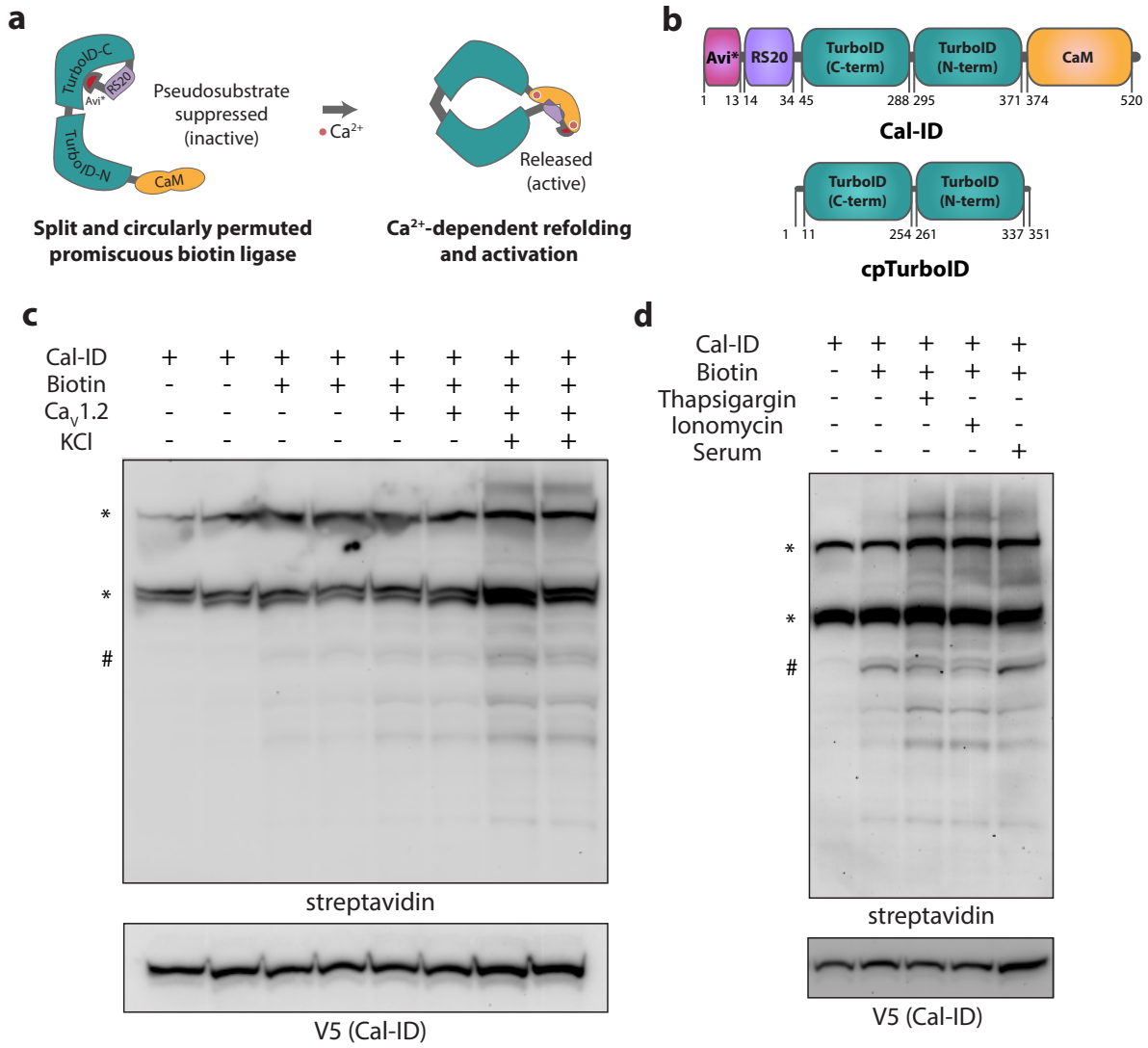

Figure 1. Cal-ID: a calcium-dependent proximal labeling enzyme.

a, A schematic diagram of Cal-ID activation. CaM: calmodulin, RS20: CaM-binding peptide. **b**, Illustrations of Cal-ID and cpTurboID domain structure. Avi*: non-biotinylatable (K to R), truncated AviTag (NDIFEAQRIEWH). **c** and **d**, Representative Cal-ID activation results in HEK293T cells. c) Biotin: 50 µM, KCl: 80 mM. 30 min incubation. d) Biotin: 50 µM, thapsigargin: 3 µM, ionomycin: 10 µM, serum: fresh media containing 10% FBS. 30 min incubation. *: endogenous biotin carrier proteins, #: self-biotinylation of Cal-ID.

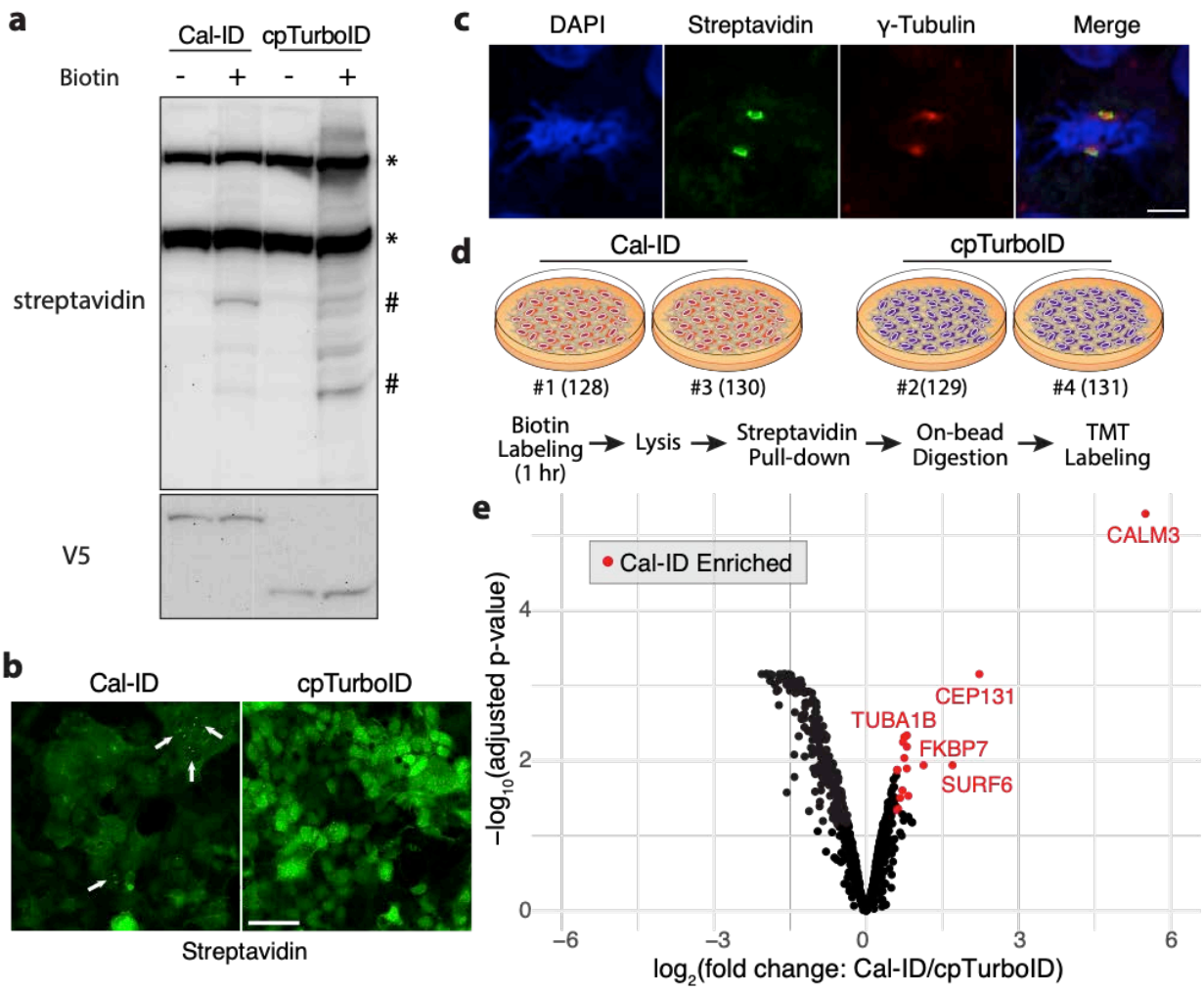

Figure 2. Identification of centrosomal calcium signaling microdomains in mitosis.

a, Representative Cal-ID and cpTurboID biotinylation results from tet-inducible stable HEK293T cell lines. Induction: 400 ng/mL (Cal-ID), 200 ng/mL (cpTurboID) doxycycline for 48 hours. Biotin: 100 µM, 1 hour incubation. *: endogenous biotin carrier proteins, #: self-biotinylation of Cal-ID. **b**, Streptavidin staining of Cal-ID- or cpTurboID-expressing stable HEK293T cell lines. Biotin: 100 µM, 1 hour incubation. Scale bar: 50 µm. **c**, Centrosomal biotinylation of mitotic cells by Cal-ID. γ-tubulin is a known marker for centrosome. Biotin: 100 µM, 1 hour incubation. Scale bar: 5 µm. **d**, A schematic diagram of TMT labeling for quantitative mass spectrometry. Isobaric tags: 128/130 (Cal-ID), 129/131 (cpTurboID). **e**, A volcano plot showing Cal-ID enriched proteins discovered by mass spectrometry. Data points: 964. Differential expression between Cal-ID and cpTurboID was analyzed using limma with FDR 5% and $\log_2$ fold change > 0.5 (significant: red).

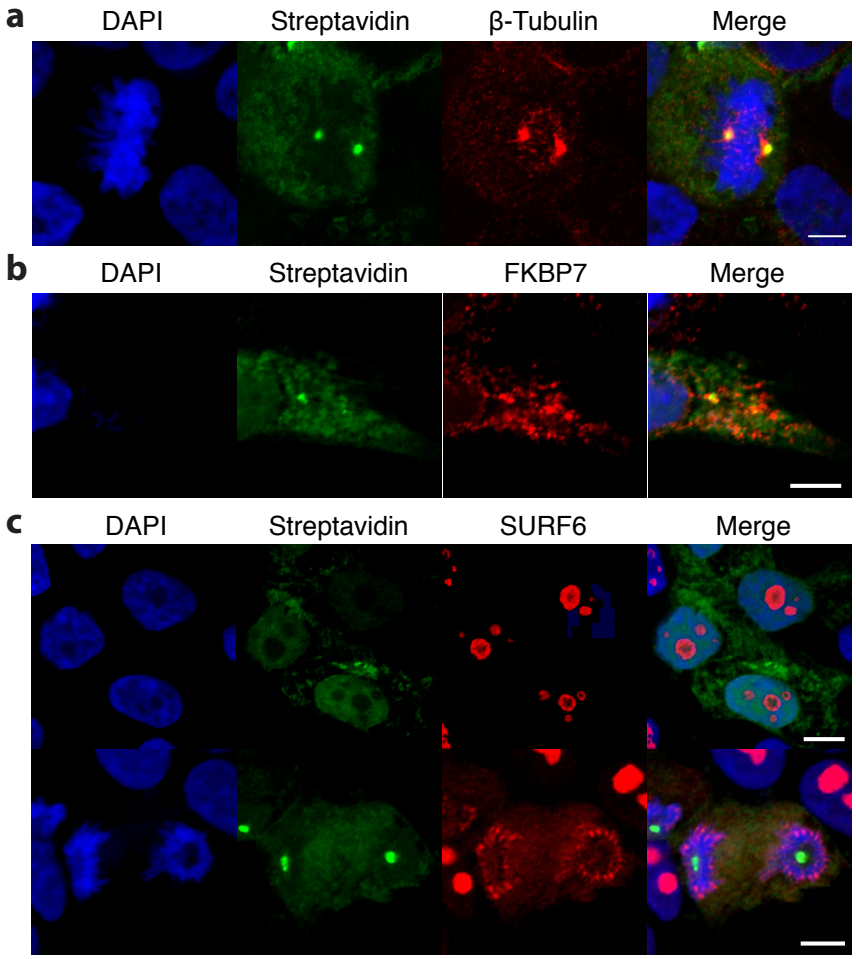

Figure 3. Visualization of Cal-ID target proteins identified by mass spectrometry

a-c, Confocal microscope images visualizing biotinylated proteins and mass spectrometry-identified target proteins in Cal-ID expressing HEK293T cells. Co-localization of streptavidin signals and a) β-tubulin found in mitotic cells, b) FKBP7 at the ER, c) SURF6 in mitotic cells. SURF6 did not show co-localization with streptavidin signals during interphase (top) but showed co-localization during mitosis (bottom). Tet-inducible stable HEK293T cells, scale bars = 5 µm.

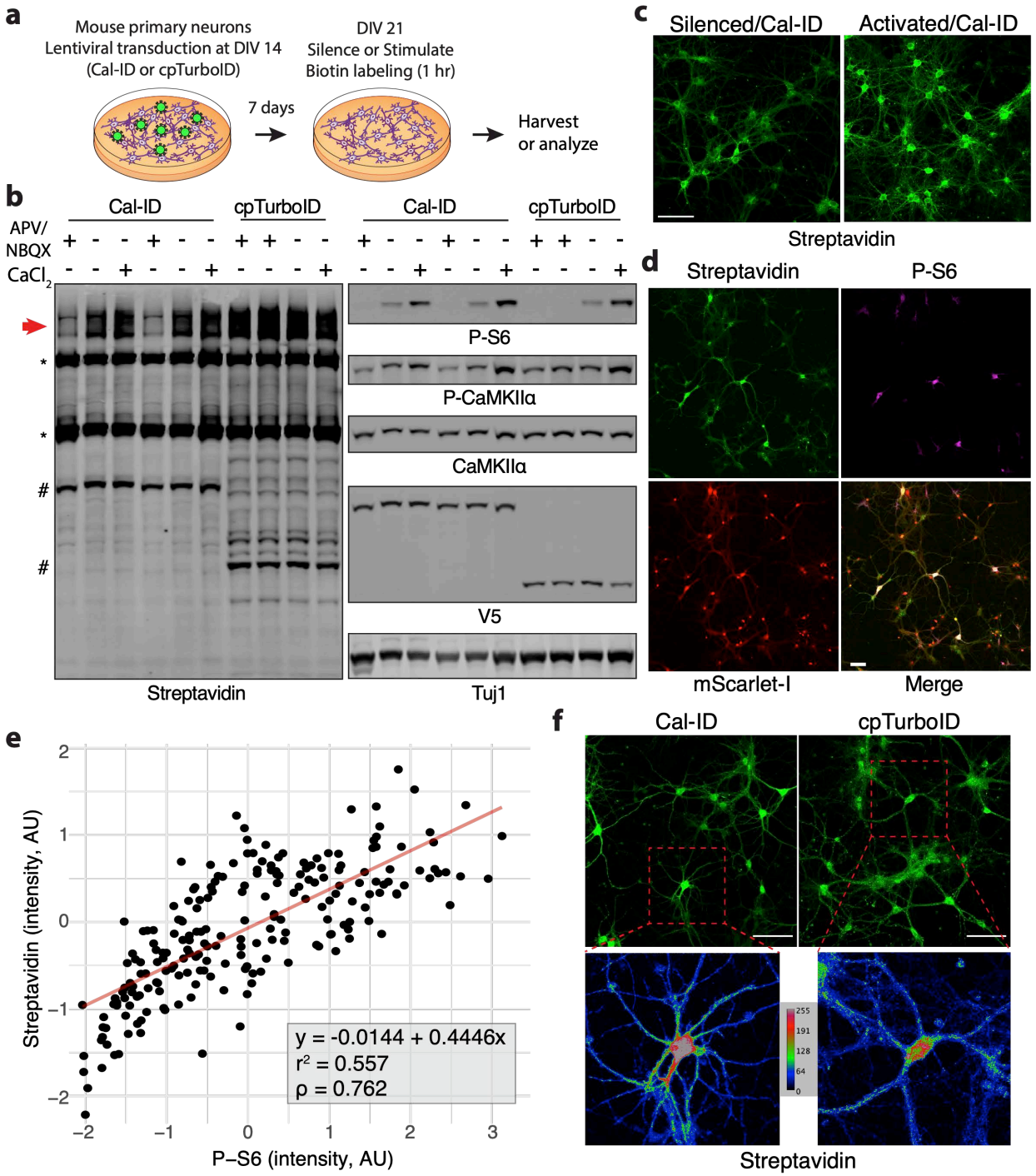

Figure 4. Cal-ID activation is associated with neuronal activity in neurons.

a, A schematic of Cal-ID or cpTurboID biotinylation in neurons. DIV: days in vitro. **b**, Cal-ID biotinylation levels are associated with neuronal activity but cpTurboID biotinylation is not. 50 µM APV (NMDAR antagonist), 10 µM NBQX (AMPAR antagonist). APV + NBQX: treated overnight. 4 mM $CaCl_2$: 1 hour. 100 µM biotin was added for 1 hour. P-S6 and P-CaMKII are activity markers. V5: Cal-ID or cpTurboID. *: endogenous biotin carrier proteins, #: self-biotinylation of Cal-ID or cpTurboID. **c**, Comparison of overall biotinylation levels between silenced and activated conditions. Silenced: 50 µM APV + 10 µM NBQX for 2 hours, activated: 25 µM bicuculline (GABAAR antagonist) for 2 hours. 100 µM biotin for 1 hour. Mouse primary hippocampal neurons. Scale bars: 100 µm. **d**, Representative images of P-S6 and streptavidin signals in mouse primary hippocampal neurons. mScarlet-I: Cal-ID expression control from Cal-ID-P2A-mScarlet-I construct. Scale bars: 50 µm. **e**, Correlation of P-S6 and streptavidin signal intensity values from d). Total 212 measurements from n = 3 (each condition). AU: arbitrary unit. **f**, Representative images of biotinylation patterns in neurons by Cal-ID or cpTurboID. Color map: signal intensity. Mouse primary hippocampal neurons. Scale bars: 100 µm.

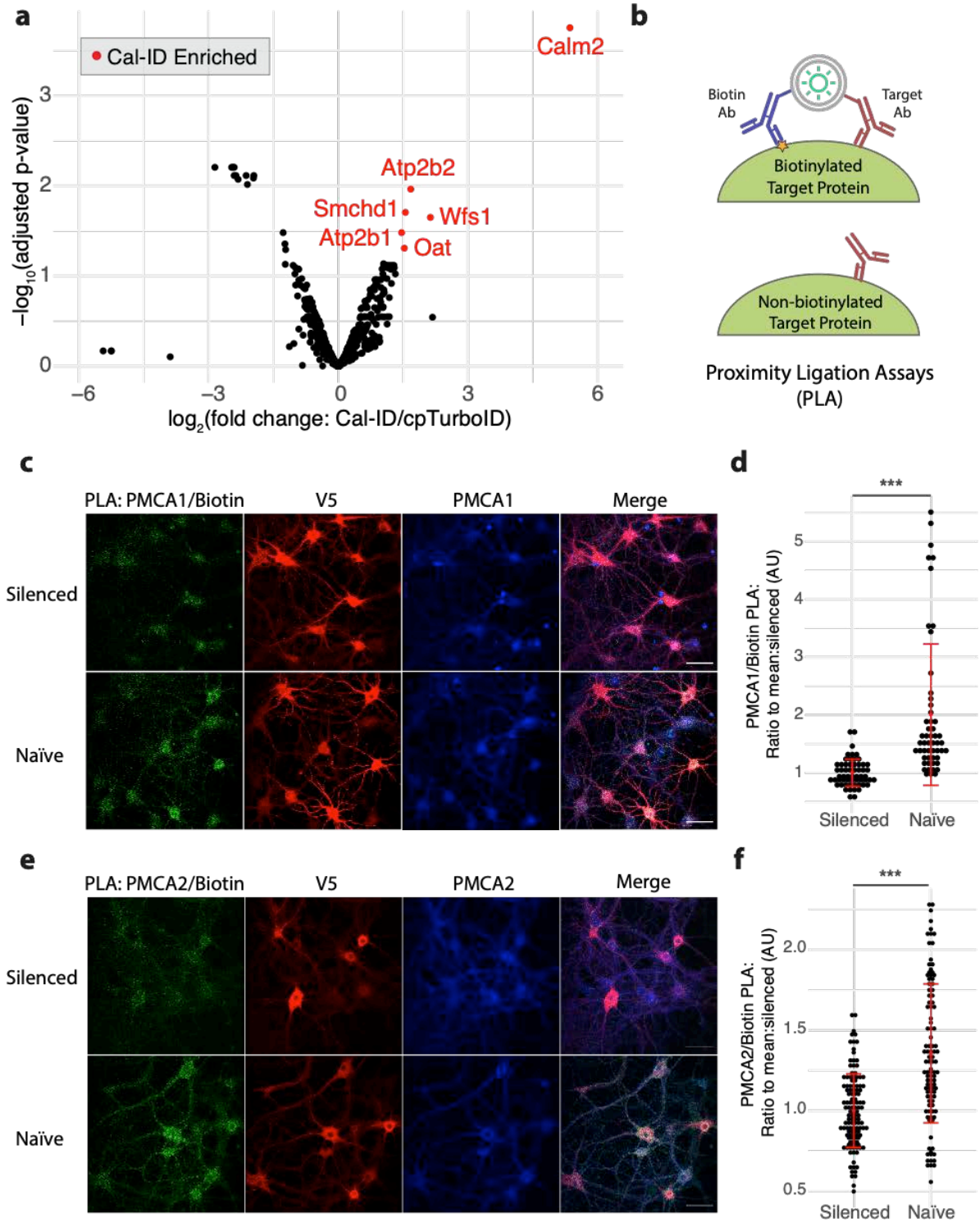

Figure 5. PMCA1/2 are associated with calcium signaling microdomains in neurons.

a, A volcano plot showing Cal-ID enriched proteins in mouse primary cortical neurons. Differential representation of 669 proteins recovered from both Cal-ID- and cpTurboID-expressing neurons was analyzed using limma with FDR 5% (significant Cal-ID enriched hits: red). Isobaric tags: 126/130 (Cal-ID), 127/131 (cpTurboID). **b**, A schematic diagram of the proximity ligation assay (PLA). **c-f**, PMCA1/2 and Biotin PLA. Silenced: 50 µM APV + 10 µM NBQX for overnight. Mouse primary hippocampal neurons, 100 µM biotin for 1 hour. c, representative images of PMCA1/Biotin PLA, d, quantification of (c), total 58 (silenced) and 53 measurements (naïve), n = 4 (each condition), e, representative images of PMCA2/Biotin PLA, f, quantification of (e), total 124 (silenced) and 105 measurements (naïve), n = 4 (each condition). Intensity ratios were calculated by normalizing raw intensity to the mean of the silenced condition for each batch. Statistical test: Student's t-test, two-tailed; error bar: mean ± SD. AU: arbitrary unit. *** $p < 0.001$. Scale bars: 50 µm.

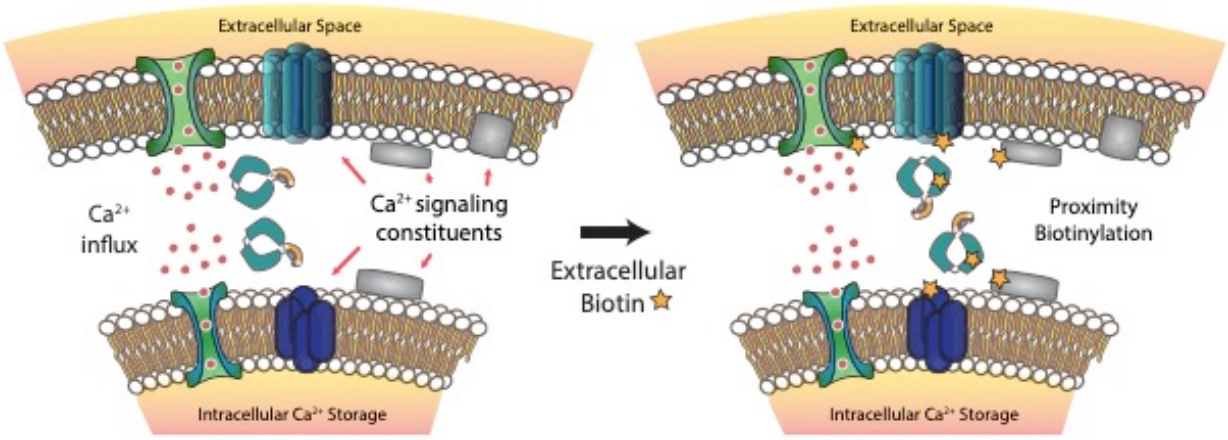

Figure 6. Cal-ID biotinylates calcium signaling microdomains in living cells.

A schematic illustration of the action of Cal-ID for the labeling of calcium signaling microdomains in living cells.

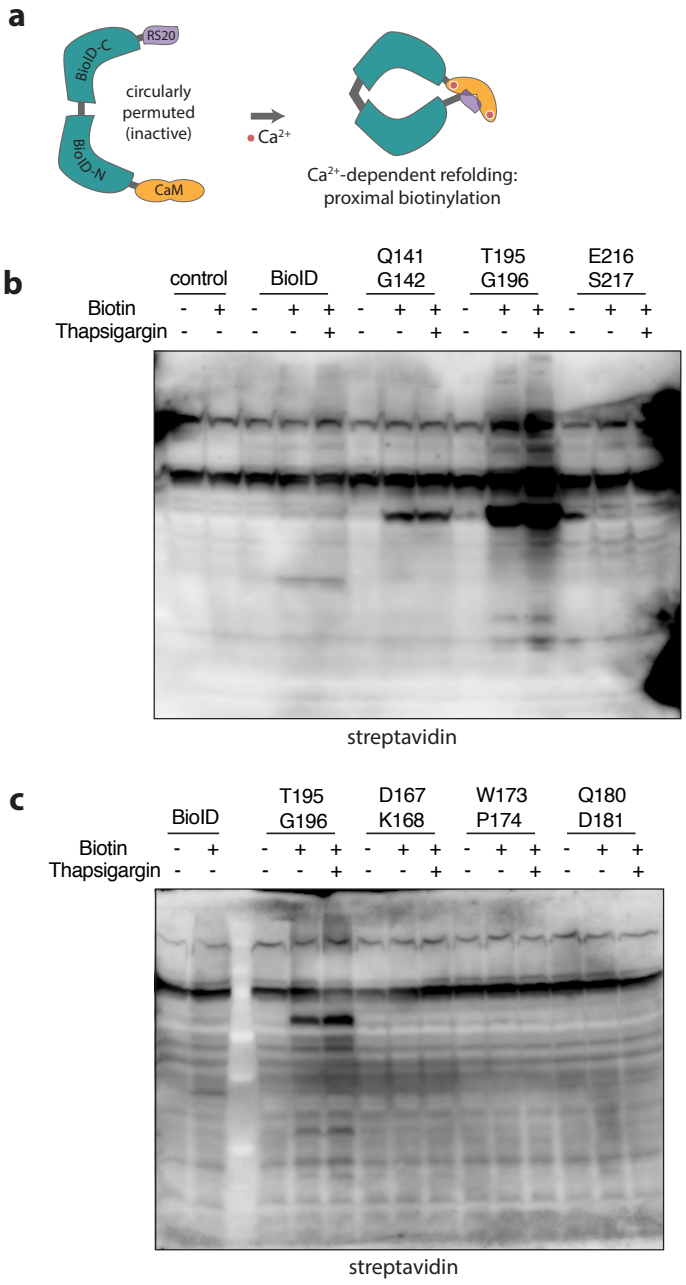

Extended Data Figure 1. BioID split site screening.

a, A schematic diagram of the Cal-ID design used to screen BioID split sites (this early version used split BioID rather than TurboID). CaM: calmodulin, RS20: CaM-binding peptide. **b and c**, Cal-ID activation results in HEK293T cells with 1 µM thapsigargin. Biotin: 50 µM, 30 min incubation. Cal-ID constructs were transfected transiently.

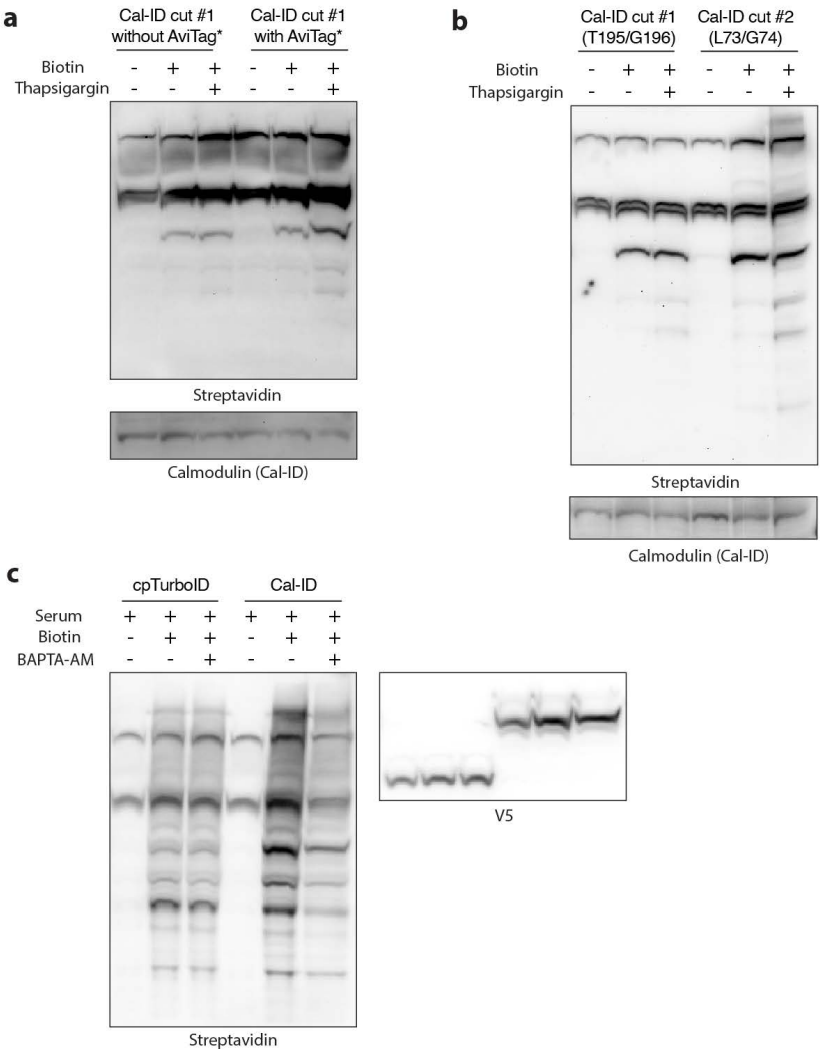

Extended Data Figure 2. Optimization of Cal-ID.

a, Representative blots testing Cal-ID (T195/G196 split) with a self-inhibitory AviTag* motif in HEK293T cells with 3 µM thapsigargin and prolonged incubation. Biotin: 100 µM, 1 hour incubation, transient transfection. **b**, Representative blots comparing Cal-ID split site variants T195/G196 and L73/G74 for short incubation. Both variants contain a self-inhibitory motif. Transient transfection in HEK293T cells, 3 µM thapsigargin, biotin: 50 µM, 15 min incubation. **c**, Representative blots showing that Ca^{2+} chelator BAPTA-AM treatment blocks Cal-ID biotinylation. Transient transfection in HEK293T cells, BAPTA-AM: 40 µM, biotin: 100 µM, serum: replacement with fresh culture media. Culture media was replaced, BAPTA-AM was treated and incubated for 3 min, then biotin was added and labeled for 30 min. V5: cpTurboID or Cal-ID.

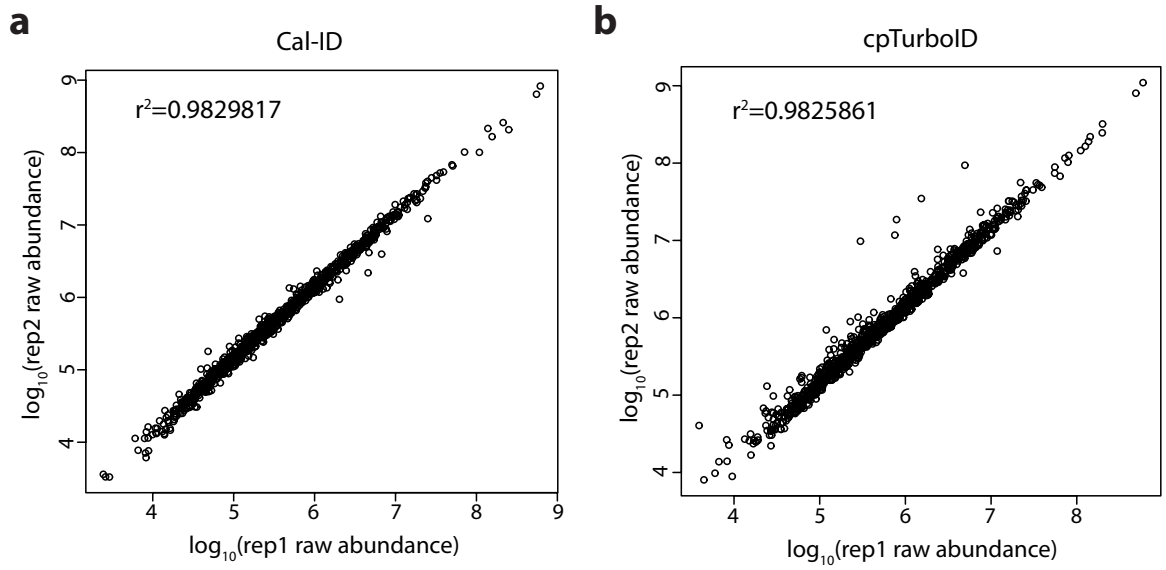

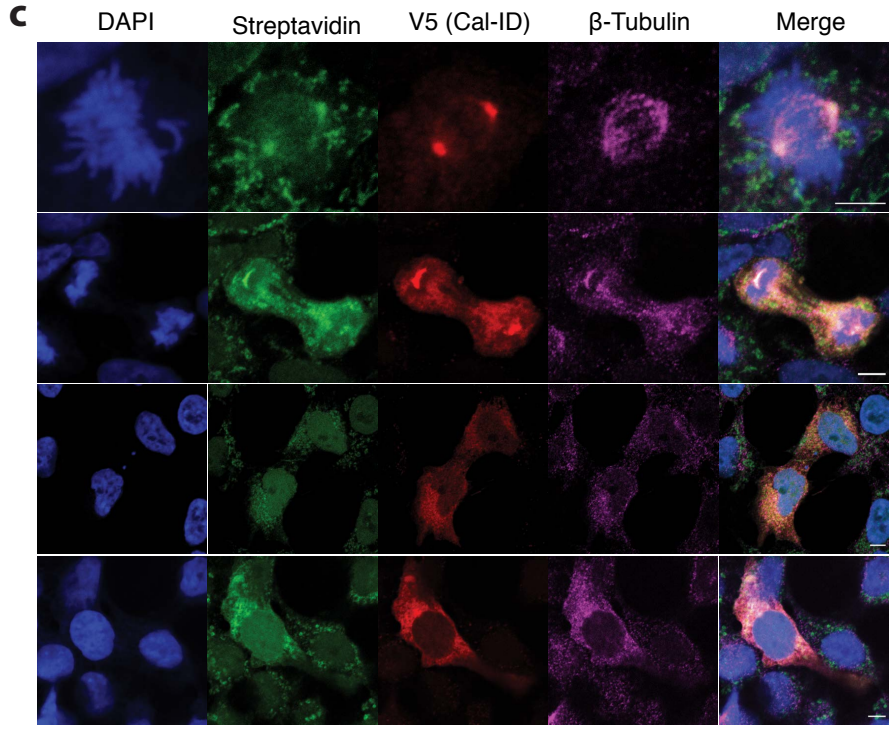

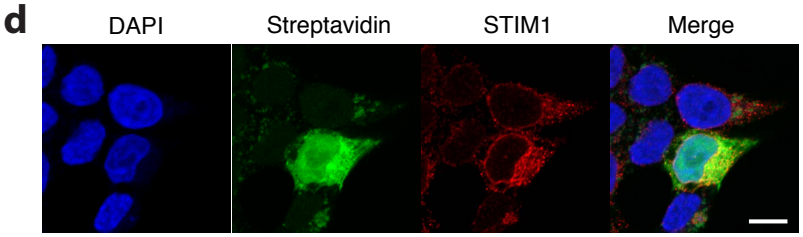

Extended Data Figure 3. Cal-ID mass spectrometry in HEK293T cells.

a and b, Scatterplots showing mass spectrometry reproducibility between biological replicates a, Cal-ID, b, cpTurboID, prepared from HEK293T stable cell lines. **c**, Representative images for β-tubulin and streptavidin co-localization and Cal-ID subcellular distribution along the cell cycle. Cal-ID localizes to centrosomes during mitosis and returns to cytosol in interphase. **d**, Representative images showing streptavidin signals and STIM1 co-localization in STIM1-activated cells. Tet-inducible stable HEK293T cells, scale bars = 5 µm, biotin: 100 µM, 1 hour incubation.

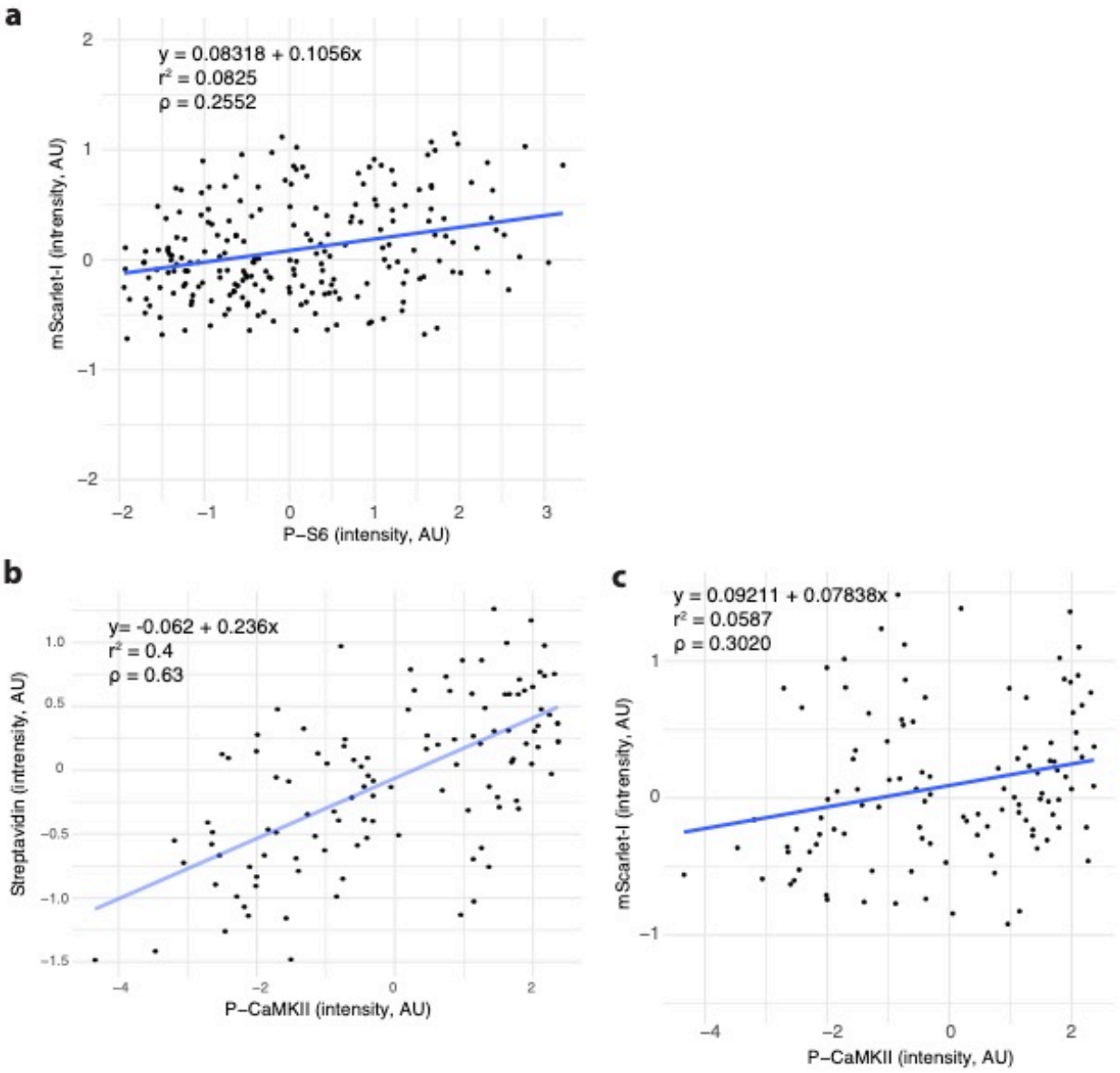

Extended Data Figure 4. Correlation between neuronal activity markers and Cal-ID biotinylation.

a, Scatterplots of P-S6 and mScarlet-I (Cal-ID expression control) signal intensity do not show a much weaker trend than streptavidin, related to Fig. 4e. **b and c**, Similar to the results from P-S6, P-CaMKII signals show a much stronger positive correlation with streptavidin signal than with mScarlet-I signals. AU: arbitrary unit.

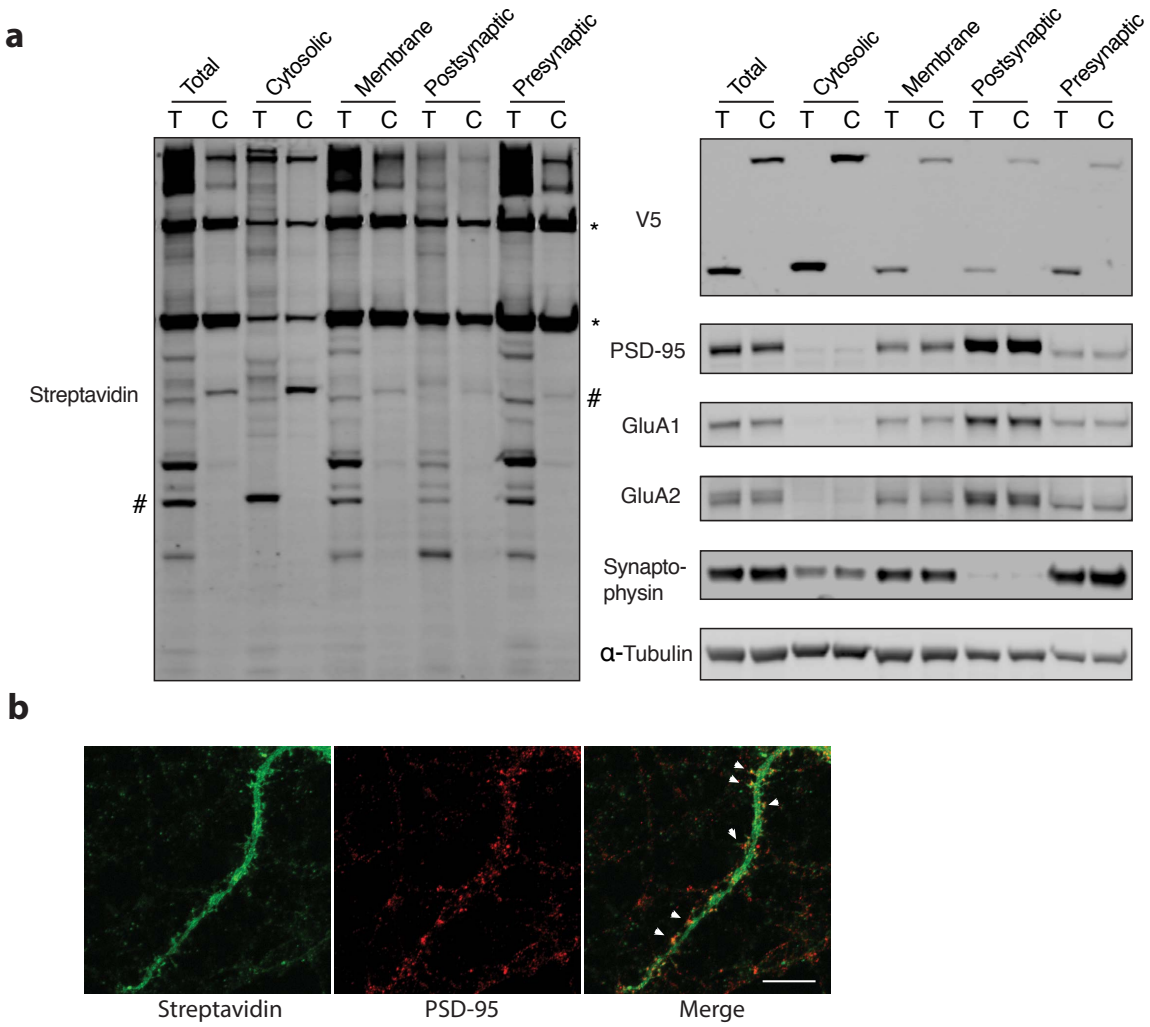

Extended Data Figure 5. Subcellular localization of Cal-ID in neurons.

a, Subcellular fractionation of Cal-ID-biotinylated primary cortical neurons. T: cpTurboID, C: Cal-ID. *: endogenous biotin carrier proteins, #: self-biotinylation of Cal-ID or cpTurboID. PSD-95, GluA1/2: postsynaptic markers, Synaptophysin: presynaptic marker, α-tubulin: loading control, V5: Cal-ID/cpTurboID epitope. b, Representative images demonstrating that Cal-ID biotinylation occurs at the postsynaptic density (PSD) (see arrows). Scale bar: 25 µm. Biotin: 100 µM, 1 hour incubation, lentiviral delivery of Cal-ID.

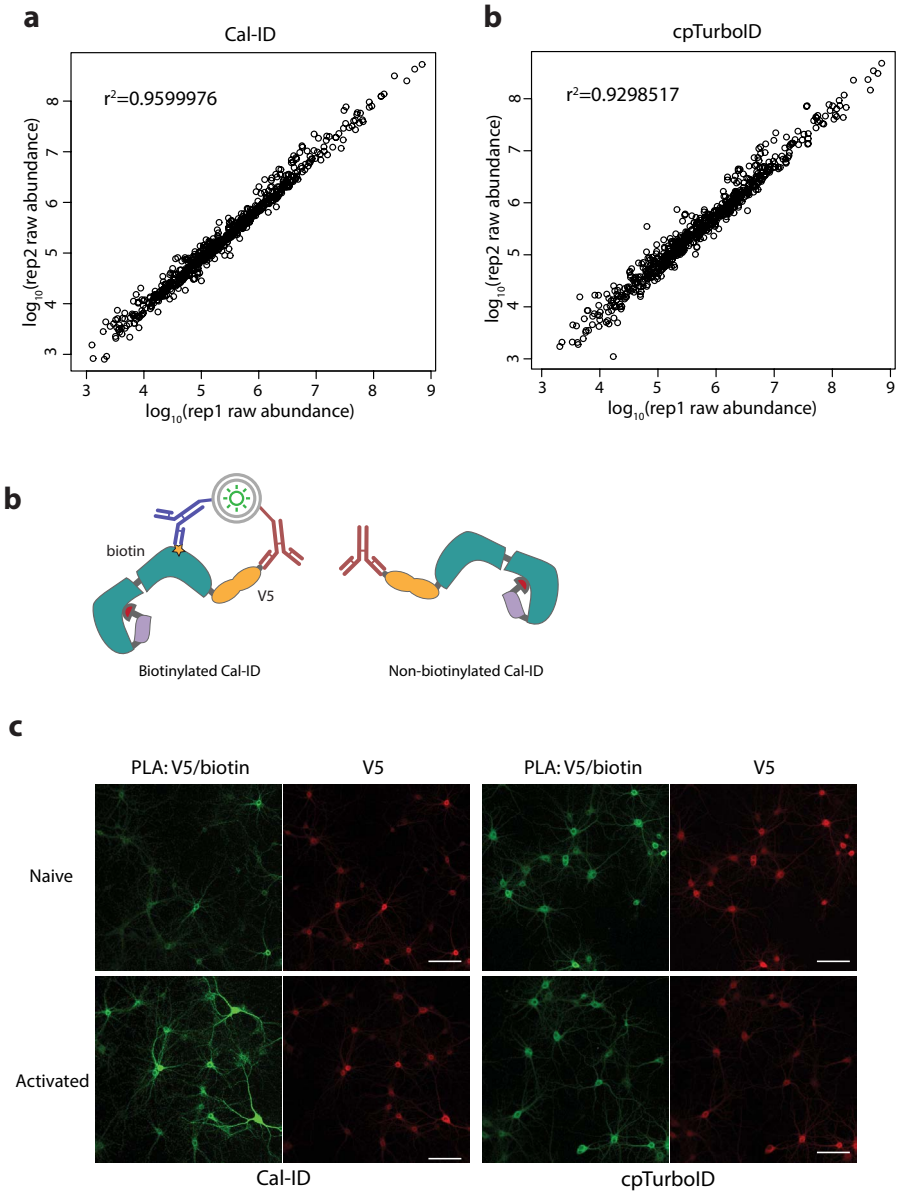

Extended Data Figure 6. Cal-ID TMT mass spectrometry from mouse primary neurons.

a and b, Scatterplots showing mass spectrometry reproducibility between biological replicates a, Cal-ID, b, cpTurboID, prepared from mouse primary cortical neurons. **b**, A schematic diagram of proximity ligation assay (PLA) to visualize self-biotinylation of Cal-ID. **c**, PLA was performed with V5 (Cal-ID) and biotin. Activated: 50 µM APV + 10 µM NBQX for overnight silencing, followed by 4 mM $CaCl_2$ along with 100 µM biotin for 1 hour. Mouse primary hippocampal neurons, lentiviral delivery, scale bar: 100 µm.